Report 78-11

A Velocity Prediction Program for Ocean racing Yachts

J.E. Kerwin

H. Irving Pratt
Ocean Race Handicapping Project

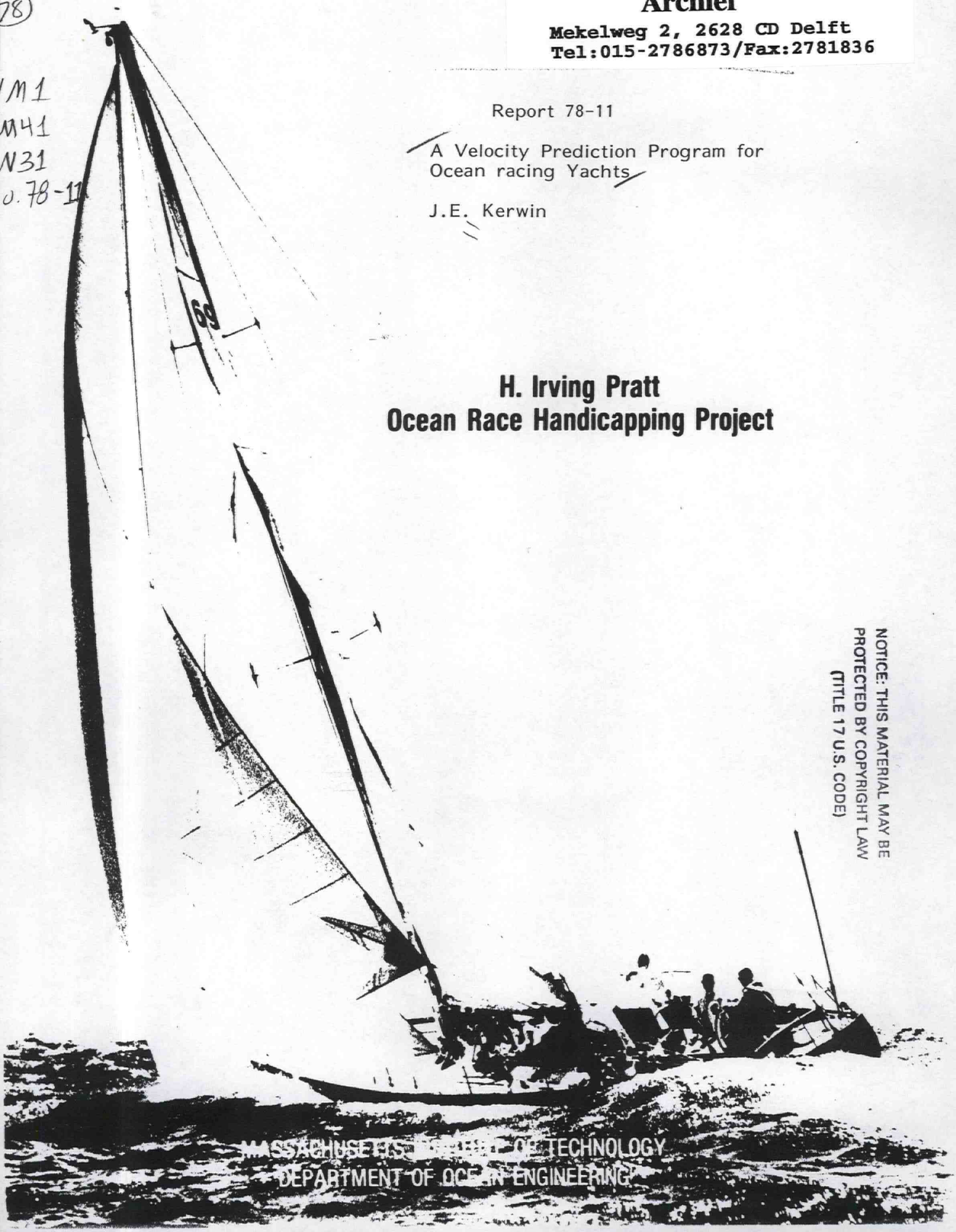

THE SOCIETY OF NAVAL ARCHITECTS AND MARINE ENGINEERS
74 Trinity Place, New York, N.Y. 10006
Paper to be presented at the New England Sailing Yacht Symposium, New London, Connecticut, January 24, 1976

A Velocity Prediction Program for Ocean Racing Yachts

Justin E. Kerwin, Associate Member, Massachusetts Institute of Technology, Cambridge, Mass. 02139

ABSTRACT

A procedure is developed to predict the sailing speed of a yacht with specified characteristics for any combination of true wind velocity and angle. The method requires as input hydrodynamic hull characteristics derived principally from towing tank tests and sail force coefficients derived from full-scale tests. The procedure permits the maximum possible generalization of these data to yachts of varying size, stability and sail area. Results are given for a geometrically similar family of yachts developed from a single parent hull.

NOMENCLATURE

a,b,c,d	Coefficients of spline-cubic approximation to upright resistance
C_F	ITTC Correlation Coefficient
C_H	Coefficient of resistance increase due to heel
C_{HO}	Sail side force coefficient at zero heel
$C_{H\phi}$	Coefficient of linear heel correction term to sail side force coefficient
C_I	Coefficient of resistance increase due to side force
C_R	Residuary Resistance Coefficient
C_{RO}	Sail driving force coefficient
$C_{R\phi}$	Coefficient of linear heel correction term to sail driving force coefficient
C_1, C_2	Coefficients in expansion of C_I in powers of ϕ^2
d_1-d_4	Coefficients in approximation to hull stability function
E	Base of mainsail
F_H	Heeling force developed by sails
F_n	Froude Number $\frac{V}{\sqrt{gL}}$
F_R	Aerodynamic driving force of sails
g	Acceleration of gravity
I	Height of fore-triangle
J	Base of fore-triangle
K	Heeling moment
L	Waterline length of hull
L_E	Effective length for computation of Reynolds Number
P	Height of mainsail
R_H	Resistance increase of hull due to heel at zero side force
R_I	Resistance increase of hull due to side force
R_n	Reynolds Number $\frac{VL_E}{\nu}$
R_S	Total hull resistance under sail, including influence of heel, leeway and side force
R_T	Total upright resistance of hull
r	Reefing function
S	Wetted surface area of hull
S_A	Sail area
V	Boat speed
V_{aw}	Apparent wind velocity
V_{mg}	Speed made good to windward
V_{tw}	True wind velocity
z_{CE}	Height of center of effort of sails above waterline, measured in vertical centerplane of yacht

z_G	Distance of yacht center of gravity below waterline
β	Leeway angle
β_{aw}	Apparent wind angle
β_{tw}	True wind angle
Δ	Displacement of hull
ρ	Mass density of water
ρ_A	Mass density of air
ϕ	Heel angle
ϕ_R	Maximum allowable heel angle

INTRODUCTION

The ultimate purpose of the Velocity Prediction Program (VPP) is to provide a means of predicting the speed of any yacht at any point of sailing in any wind velocity. The average speeds of a hypothetical or real fleet over a prescribed course obtained by the VPP can provide one basis for the evaluation of existing or proposed time allowance and rating formulae. In this way, the influence of the basic speed-producing factors of a yacht can be studied without the disturbing influences of weather, chance and sailing skill which are inevitably present in real race data. Moreover, the VPP can be used directly to develop a handicapping system. An example of such an application may be found in [1].

In its present form, the VPP requires as input the nondimensional resistance characteristics of the hull and the nondimensional driving and side force characteristics of the sails. While a large quantity of towing tank data exists, differences due to scale effects and due to variations in specific testing procedures at different facilities make such data of questionable value in the handicapping problem. However, there are two types of tank tests which are useful. The first is simply the use of the tests of a single model to obtain the performance of a geosim family of yachts of different sizes. In this case, the relative performance of full-size yachts of varying size can be predicted with far greater confidence than the absolute performance of a single prototype. If the model test covers a sufficiently wide range of conditions, the performance of a fleet of not only varying size, but varying sail area and stability can be established.

The second type of test is a systematic series of model tests, all done in a single facility on similar size models using strictly controlled test procedures. In this case, the influence of those basic speed-producing hull parameters which are least subject to uncertain scale effects can be incorporated in full-scale performance predictions. Such parameters include, for example, displacement/length ratio, length/beam ratio, and prismatic coefficient.

The design and testing of such a series is presently underway in a cooperative program between the MIT/NAYRU Ocean Race Handicapping Project and the Shipbuilding Laboratory of the Delft University of Technology. These tests are being made with relatively large models with a length overall of 7 feet and an average displacement of 90 pounds. In addition, Panel H-13 of the Society of Naval Architects, with the cooperation of Hydronautics, Incorporated, and the Davidson Laboratory, is sponsoring the testing of a 22-foot and 4.8-foot model of the parent hull of the systematic series. When completed, these programs are expected to provide an extensive and reliable data base for the VPP.

The prediction of yacht sailing performance from tank tests requires knowledge of the driving and side force characteristics of the sails. For the past 40 years, practically all such predictions have been based on the classical GIMCRACK sail coefficients developed by Davidson [2]. These coefficients are limited to optimum close-hauled apparent wind angles, so that no information is provided for reaching and running conditions. In addition, the geometry of GIMCRACK's rig differs considerably from that of a current ocean racing yacht and, of course, sailmaking technology has advanced significantly since 1936.

There are three possible approaches to determining sail force coefficients for ocean racing yachts:

1. Aerodynamic Theory [3],[4];
2. Wind Tunnel Tests of a Model Rig [5],[6],[7];
3. Full-Scale Sailing Trials combined with towing tank tests of the hull [2],[8],[9].

Aerodynamic theory provides a rational means of estimating the effect of rig proportions on windward sailing performance. However, present analytical methods cannot be expected to provide correct results for off-wind sailing conditions. Wind tunnel would appear to be the logical counterpart to tank tests of a hull. However, there are

important differences which severely limit the usefulness of wind tunnel tests, particularly from the point of view of obtaining representative sail force coefficients for ocean race handicapping. While a yacht has one hull of fixed and precisely known geometry, it is likely to have twenty or more sails set in various combinations, each with infinitely varying and generally unknown shape. These sails cannot be reproduced by deformable fabric models, nor is it practical to measure and reproduce as a rigid model the large number of geometries necessary to characterize an ocean racing yacht. Even if this were possible, wind tunnel wall effects introduce large errors in the measurement of off-wind sailing conditions.

This therefore leaves the full-scale sailing trial, preferably under racing conditions, as the only practical means of obtaining the complete characterization of the rig of an ocean racing yacht for all points of sailing and for all wind velocities. While individual measurements obtained in this way can contain large random errors associated with non-laboratory-controlled conditions, suitably averaged data can be considered to be reliable.

This approach was used to analyze data recorded on BAY BEA during the 1974 SORC [7], and on STANDFAST during the 1974 racing season in Europe [8].

THE VPP MATHEMATICAL MODEL

Hull Resistance

For a hull of specified size and geometry the total resistance under sail R_S and side force $F_H \cos\phi$ are functions of speed, V, leeway angle, β, and heel angle, ϕ.[1] The resistance R_S is defined as the force in the direction of the velocity of the yacht, while $F_H \cos\phi$ is the horizontal component of the force, at right angles to the velocity. In [7] the functions R_S and $F_H \cos\phi$ were approximated by polynomials in these three independent variables, using the procedure developed at M.I.T. in 1964 [9]. However, since we are principally concerned with equilibrium between sail and hull forces, it is more efficient to eliminate leeway as a parameter and to consider that the resistance is a function of speed, side force and heel angle. The remaining equation relating side force to leeway angle is therefore unnecessary in establishing the equilibrium speed of the yacht.

We can then consider the total resistance R_S to consist of three additive terms:

a) Upright resistance with zero side force; R_T.

b) Resistance increase due to heel at zero side force; R_H.

c) Resistance increase due to side force; R_I.

Upright Resistance. Upright resistance, for a fixed size, is a function of speed alone. The effect of size for geometrically similar hulls may be obtained in the usual way in accordance with Froude's hypothesis:

$$R_T = \frac{1}{2}\rho S V^2 \left[C_F(R_n) + C_R(F_n)\right] \qquad (1)$$

where

$$C_F = \frac{0.075}{(\log_{10}(R_n) - 2)^2} \qquad (2)$$

is the ITTC correlation coefficient expressed as a function of the Reynolds Number

$$R_n = \frac{V L_E}{\nu} \qquad (3)$$

and C_R is the residuary resistance coefficient which is a function of Froude Number

$$F_n = \frac{V}{\sqrt{gL}} \qquad (4)$$

If we take the effective length for frictional resistance as 70% of the waterline length

$$L_E = 0.7L \qquad (5)$$

we can rewrite (2) in terms of dimensional quantities immediately available for computation

$$C_F = \frac{\ln\left(\frac{118223LV}{\nu}\right) - 2}{2.302585}^2 \qquad (6)$$

In this case, the waterline length L is in feet, the speed V is in knots and the quantity ν is 10^5 times the kinematic viscosity of sea water in units of ft^2/sec.

The residuary resistance coefficient, C_R, is assumed to be known at eight values of speed-length ratio

$$\frac{V}{\sqrt{L}} = 0.4(0.2)1.8 \qquad (7)$$

---

[1] The notation $F_H \cos\phi$ is generally used to denote the aerodynamic side force developed by the sails. To simplify notation, the same symbol is used here to denote the equilibrating hydrodynamic side force acting on the hull.

where V is again in knots and L is in feet. A program has been developed to obtain this information from a towing tank test by a least-squares spline cubic curve fitting technique, and a typical result is given in [8]. However, the choice of this form of input makes it possible to use data from practically any source.

For any desired size hull, we can use (1) to compute eight values of R_T at speeds given by (7). Considering the point at the origin, which is, of course, zero, we have a total of nine points. The resistance curve is assumed to be a spline function passing through these nine points, with a further constraint of zero slope at the origin. Let V_j be the "base" speeds corresponding to speed length ratios of 0, .4, .6, ... 1.8. A particular speed V falls in the jth interval where

$$V_j \leq V < V_{j+1} \tag{8}$$

while the last interval corresponding to j = 8 extends from V_7 to arbitrarily large speeds. The resistance curve in the jth interval is therefore a cubic of the form

$$R_T(V) = a_j(V-V_j)^3 + b_j(V-V_j)^2 + c_j(V-V_j) + d_j \tag{9}$$

The coefficients $a_j, b_j \ldots d_j$ are obtained by requiring that the approximating cubics pass through the tabular points and that the slopes and curvatures are continuous at each of their junctures. An upright resistance curve defined in this way is illustrated in Fig. 1.

This procedure has a number of advantages over the polynomial approximations used previously [7]. A better fit is obtained, particularly for resistance curves with the typical sudden turning upward at "hull speed," and the proper behavior both at low and at high speeds can be obtained. In addition, the evaluation of (9) is very rapid once the coefficients have been obtained. Hence, this procedure is particularly efficient if a large number of resistance computations are to be made from a single curve.

Resistance Due to Heel and Side Force

The resistance increase due to heel at zero side force is governed principally by the alternation of hull shape, which may or may not be large. Presumably a narrow yacht with relatively circular sections would experience practically no change in resistance with heel, while a yacht with large beam amidships and fine ends

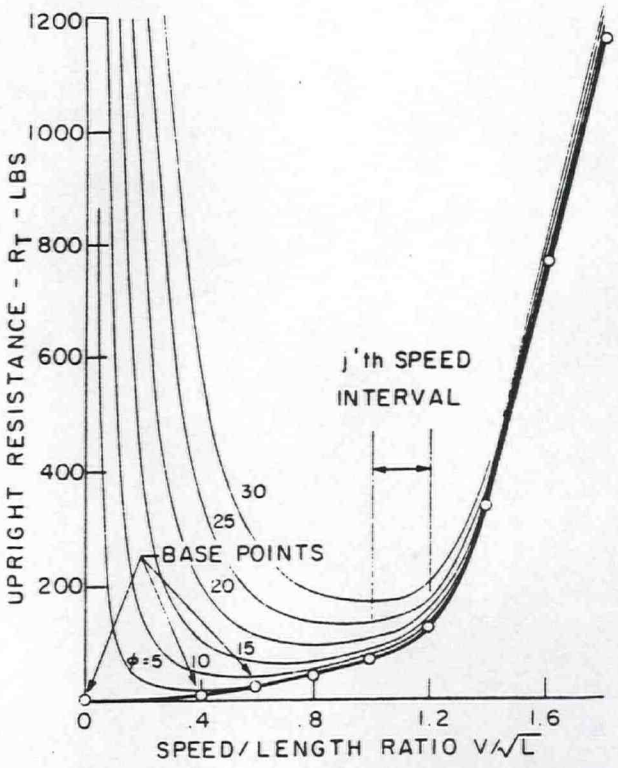

Figure 1. Upright resistance curve.

would be expected to show a significant resistance increase at high speeds due to reduced section area at the ends. In any event, we must resort to a curve fitting procedure of model resistance data, using a suitable function of heel and speed. The simplest possible function is

$$R_H = \frac{1}{2}\rho S V^2 \phi^2 C_H \tag{10}$$

where the heeled resistance coefficient is independent of Froude Number, and increases quadratically with heel angle. Alternatively, the function C_H could be considered to be a linear or parabolic function of Froude Number, with the possible addition of higher power, of heel angle. The coefficients of any such approximation, as we shall see later, can be obtained from a least-squares fit to model test data.

The resistance increase due to side force can be readily identified as induced drag, which is principally a function of the effective aspect ratio of the hull-keel combination and of the square of the heeling force coefficient.

$$R_I = \frac{1}{2}\rho S V^2 C_I(\phi, F_n) \quad \frac{F_H^2}{(\frac{1}{2}\rho S V^2)^2} \tag{11}$$

where the coefficient C_I depends on shape, heel and Froude Number. For low values of the Froude Number the free surface becomes effectively a rigid plane so that the coefficient C_I can be regarded as a function of heel only. Hence the simplest possible

approximation to hull-induced drag involving the effect of heel is

$$R_I = \frac{(C_1 + C_{2d}{}^2)\, F_H{}^2}{\frac{1}{2}\rho S V^2} \qquad (12)$$

where the coefficients C_1 and C_2 must be obtained by a fit to experimental data. A further refinement, as with the expression for the heeled resistance, would consist of replacing C_1 and C_2 by suitable functions of Froude Number, and heel angle.

It is important to note the presence of V in the denominator of (12). For a fixed side force and heel angle, the induced drag increases with decreasing yacht speed, and, in fact, becomes infinite at zero speed. This characteristic is well confirmed by model tests [8].

The coefficients C_H, C_1 and C_2 can be obtained by a least-squares fit to model data. At the time of writing, this has been done for the BAYBEA hull tested at M.I.T., for the STANDFAST 40 tested at Delft, and for the first five models of the systematic series underway at Delft. In all cases, the root-mean-square deviation between the predicted and measured model resistance is between 3 and 5 percent. It has been found that the addition of terms involving Froude Number and/or higher powers of heel angle do not result in a significant reduction in the rms error. We conclude, therefore, that a significant part of the rms deviation is due to inherent testing error rather than a limitation of the mathematical model. This question is studied in somewhat more detail in [8].

Hull Stability

The hydrodynamic righting moment of the hull taken about a specified reference point is a function of heel angle, speed and side force. The primary term is, of course, the linear hydrostatic righting moment. This is either measured directly by means of an inclining experiment, or computed from known geometric characteristics of the hull and the vertical position of the yacht's center of gravity. However, a yacht hull form generally displays a noticeable reduction in stability at high speed due to a decrease in beam amidships caused by its own wave profile. In addition, a nonlinear dependence of righting moment with heel is significant at large angles.

A satisfactory approximation to the righting moment function with respect to an origin at the waterline is

$$K(\phi) = \Delta L\phi\{d_1 + d_2 F_n + d_3\phi\} + d_4 L F_H + \Delta z_G \sin\phi \qquad (13)$$

where d_1-d_4 are nondimensional constants dependent only on hull shape. The quantity $\Delta L\phi d_1$ is the linear hydrostatic righting moment, while $d_1 L$ is the metacentric height for the yacht with the center of gravity at the waterline. The constants d_2 and d_3, which are generally negative, provide the speed and nonlinear heel effects just discussed. The quantity $d_4 L$ represents the distance of the center of effect of the heeling force below the waterline. The last term, $\Delta z_G \sin\phi$, is the moment of the yacht's weight about an axis at the waterline, when z_G is the distance of the center of gravity below the waterline.

The unknown coefficients in (13) may be found by least-squares from towing tank tests, provided that the model center of gravity and the applied heeling moment for each run is recorded. If these data are not available, it is reasonably accurate to determine d_1 from the IOR inclining test and to set d_2 and d_3 equal to zero. Since the initial static stability in racing trim exceeds the IOR value due to the added weight of crew, stores and liquids, this tends to compensate for the error introduced by neglecting d_2 and d_3.

Sail Forces

The resultant sail force is assumed to consist of a driving force F_R acting in the direction of the velocity of the yacht, and a heeling force F_H acting at right angles to the plane formed by F_R and the vertical axis of the yacht. The side force is therefore $F_H \cos\phi$, acting at a distance z_{CE} above the waterline, measured along the vertical axis of the yacht.

These forces can be expressed in terms of nondimensional sail force coefficients

$$F_R = \frac{1}{2}\rho_A S_A V_{aw}^2 C_R$$
$$F_H \cos\phi = \frac{1}{2}\rho_A S_A V_{aw}^2 C_H \qquad (14)$$

where ρ_A is the density of air, S_A is a suitably defined sail area and V_{aw} is the apparent wind velocity. As indicated in the introduction, values of C_R and C_H were first given by Davidson [2] based on tests with the yacht GIMCRACK. The results plotted in Figs. 2 and 3 were obtained from an analysis of data recorded on BAYBEA during the 1974 SORC [7] and may be considered representative of a current sloop rig. Data subsequently analyzed from the yacht STANDFAST obtained with

more elaborate recording instrumentation combined with extensive tank tests [8] yielded results very similar to the BAYBEA sail coefficients.

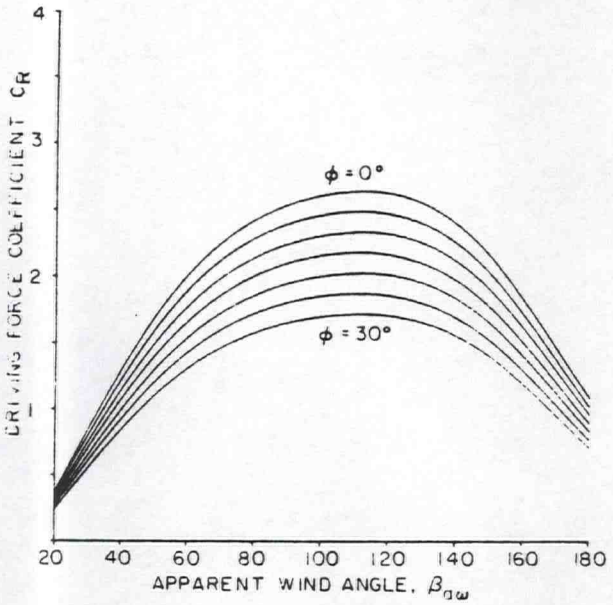

Figure 2. Driving force coefficients for 5 degree increments of heel angle.

These coefficients are assumed to be the product of a linear function of heel angle and a spline-cubic function of apparent wind angle, β_{aw}

$$C_R = C_{RO}(\beta_{aw})[1 + C_{R\phi}\phi]$$

$$C_H = C_{HO}(\beta_{aw})[1 + C_{H\phi}\phi] \qquad (15)$$

The characteristic area in (14) is taken, for simplicity, to be the area of the fore and main triangles

$$S_A = \frac{1}{2}[IxJ + PxE] \qquad (16)$$

which is generally less than the actual area of the sails set. The effect of actual sail area and the nature of the particular sails set at various wind angles is incorporated in the sail coefficients.

The coefficients in Figs. 2 and 3 were developed from data taken principally in light and moderate winds with the maximum sail area set and trimmed optimally for these conditions. In actual practice, once the wind velocity increases above some minimum value, sail force coefficients are continually reduced with increasing wind strength through sail shape control, reefing and sail changes.

In the present program, this phenomenon is idealized by defining a reefing function, r, such that

$$(S_A)_{effective} = r^2 S_A \qquad (17)$$

$$(z_{CE}+d_4L)_{effective} = r(z_{CE}+d_4L) \qquad (18)$$

Since sail forces are proportional to the product of the sail coefficient and the sail area, it obviously does not matter whether one considers that

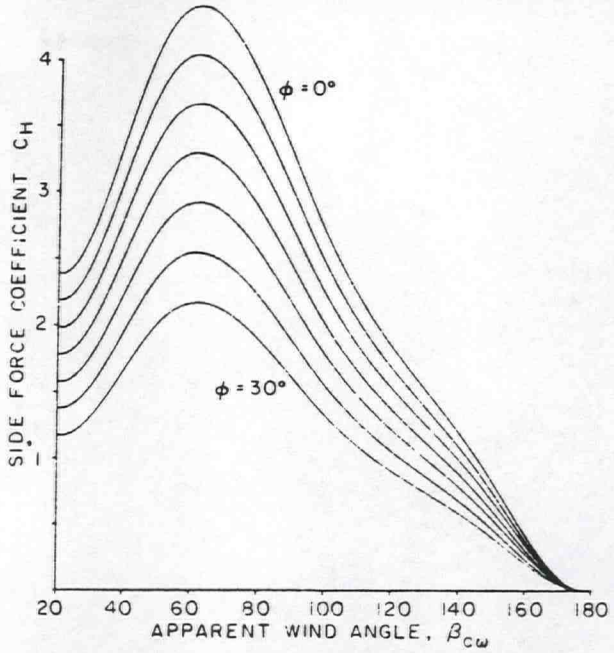

Figure 3. Side force coefficients for 5 degree increments of heel angle.

the sail coefficient is reduced by sail shape control or that area is actually reduced by reefing. We are making the assumption, however, that the driving and side forces are being affected in the same way. If the sails are uniformly flattened to reduce their lift coefficient, their induced drag will decrease, thus increasing the ratio of driving to side force. However, if the upper part of the sails are unloaded to reduce heeling moment, or if the span of the sails is reduced by reefing, induced drag will increase and the ratio of driving to side force will decrease. It therefore does not seem unreasonable to consider that, on an average, the two effects will cancel.

The height of the center of effort also depends on the particular details of the method of reducing sail forces. Since the distance from the center of effort of the keel to the lowest part of the sails certainly does not decrease with reefing, the quantity $z_{CE} + d_4L$ probably decreases at a slower rate than r. It is planned, therefore, to modify (18) in the future, possibly replacing r by $r^{1/2}$.

The degree of reefing is determined in such a way as to maximize speed, with the constraint that the heel angle does not exceed 30 degrees. The details of this optimization procedure are given subsequently.

ITERATIVE PROCEDURE TO OBTAIN EQUILIBRIUM SAILING CONDITION

To obtain the equilibrium condition for a given value of true wind speed V_{tw}, and true wind direction, β_{tw}, we must solve a coupled set of four nonlinear algebraic equations. The first three,

a) Hull resistance

b) Hull stability

c) Sail forces,

have been developed in the preceding sections. The fourth equation is simply the wind triangle, relating apparent and true wind velocities and directions.

It is essential for the iterative procedure for the solution of these equations to be as efficient as possible since it is anticipated that enormous numbers of such calculations will be necessary during the course of analysis of handicapping systems. It is also important for the yacht speed to converge to a fine tolerance. Speed differences resulting from small changes in yacht characteristics must be predicted with sufficient precision to enable comparison with handicapping system expectations.

A simplified flow diagram for the iterative solution is given in Fig. 4. The outermost loop consists of computation of performance for true wind velocities of 5, 10, 12, 15, 20 and 30 knots. For each true wind velocity, computations are made for 17 true wind angles starting with a dead run and ending with the angle for maximum speed made good to windward. For each true wind angle, the quantities $V_{tw} \sin \beta_{tw}$ and $V_{tw} \cos \beta_{tw}$ are computed for use later in the wind triangle expression. Since these are unchanged in the iterative steps to follow, this saves some computer time.

The iteration begins with an initial guess for boat speed. For the dead run, this is taken to be either half the true wind velocity or a speed/length ratio of 1.5, whichever is less. For all subsequent wind angles at the same wind speed, the initial guess for boat speed is the final equilibrium speed obtained for the preceding wind angle. In this way, use is made of preceding information to minimize the number of iterations.

With an assumed boat speed, we can solve the wind triangle

$$V_{aw}^2 = (V_{tw} \sin \beta_{tw})^2 + (V_{tw} \cos \beta_{tw} + V)^2$$

$$\beta_{aw} = \tan^{-1} \frac{V_{tw} \sin \beta_{tw}}{V_{aw}} \qquad (19)$$

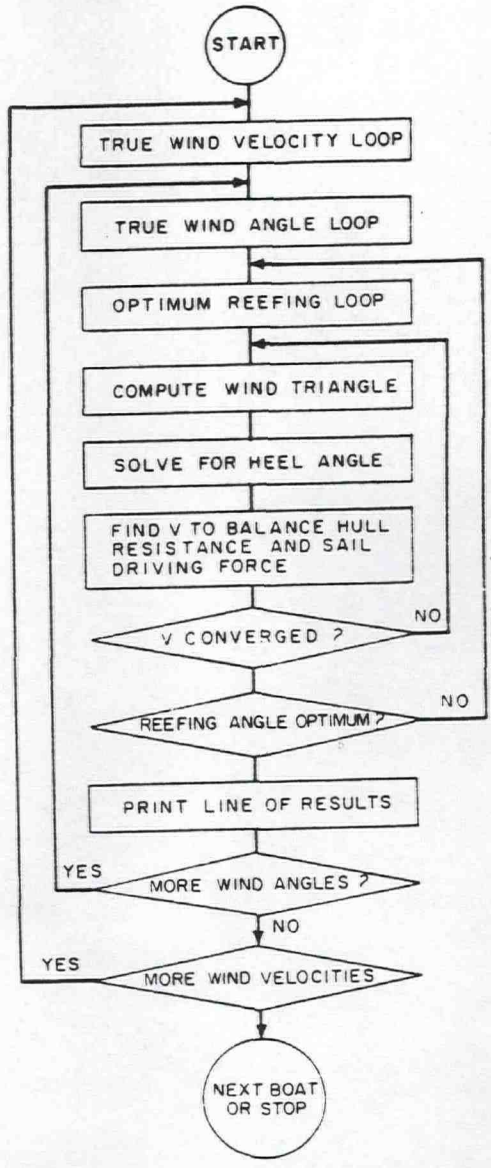

Figure 4. VPP simplified flow diagram.

The inevitable ambiguity of quadrants in the inverse tangent function enters in here, so that we must increase β_{aw} by 180° if $(V_{tw} \cos \beta_{tw} + V) < 0$. Finally, to avoid an overflow if the latter function is equal to zero, the arc tangent computation is skipped and β_{aw} is set equal to 90° if $|V_T \cos \beta_{tw} + V| < 0.001$.

With β_{aw} known, we can now obtain the upright sail coefficients C_{RO} and C_{HO}. To save time, these are obtained by linear interpolation from an input array tabulated at one degree intervals of apparent wind angle starting with twenty degrees. The tabular

values bracketing any given β_{aw} may be found directly by an index defined as the largest integer $\leq (\beta_{aw}-19)$. This avoids a table search which is always computationally inefficient.

The next step is to solve for the heel angle, ϕ, subject to the constraint that it not exceed a specified maximum, which is initially taken to be 22 degrees. Two possibilities exist:

a) The heel angle with full sail, r = 1, is less than the assumed optimum heel angle. In this case, the heel angle is obtained by a recursive solution of the moment equilibrium equation

$$\phi = \frac{\frac{1}{2}\rho_A r^3 S_A V_{aw}^2 (z_{CE}+d_4 L)\{C_{HO}(\beta_{aw})[1+C_{H\phi}\phi]\}}{\Delta L(d_1+d_2 F_n+d_3\phi+d_5\frac{\sin\phi}{\phi})\cos\phi} \qquad (20)$$

starting with an initial value of $\phi = 0$. Since the influence of ϕ on the right-hand side of (20) is very weak, convergence to a specified tolerance of 0.1 degrees is very rapid. The reefing ratio, r, appearing in (20) is, by definition, unity in this case.

b) The heel angle with full sail would exceed the assumed optimum heel angle. In this case, the heel angle is set equal to the reefing angle ϕ_R, and (20) is solved directly for the reefing ratio

$$r = \left[\frac{[\Delta L\phi_R(d_1+d_2F_n+d_3\phi_R)+\Delta z_G \sin\phi_R]\cos\phi_R}{\frac{1}{2}\rho_A S_A V_{aw}^2 (z_{CE}+d_4 L)[C_{HO}(1+C_{H\phi}\phi_R)]}\right]^{1/3} \qquad (21)$$

We now have values for the relative wind strength, V_{aw}, relative wind angle, β_{aw}, and heel angle, ϕ. The sail driving and side forces are therefore known

$$F_H \cos\phi = r^2 \tfrac{1}{2}\rho_A V_{aw}^2 S_A C_{HO}[1+C_{H\phi}\phi]$$

$$F_R = r^2 \tfrac{1}{2}\rho_A V_{aw}^2 S_A C_{RO}[1+C_{R\phi}\phi] \qquad (22)$$

These expressions are valid whether or not reefing is present as a consequence of the definition of the reefing ratio r.

We are now ready to enter the forces from (22) and the heel angle into the hull drag function in order to obtain the equilibrium speed. This is still not the final solution since the quantities obtained at this stage are dependent on the initial guess of boat speed, which will not generally be the same as the speed found for hull drag equilibrium. Hence, once we complete the next iteration, it will still be necessary to repeat the entire process a number of times until the assumed boat speed used in obtaining the apparent wind agrees with the boat speed obtained from equilibrium of sail and hull forces.

The solution for boat speed for a given drag can be seen in graphical form in Fig. (5). It is important to

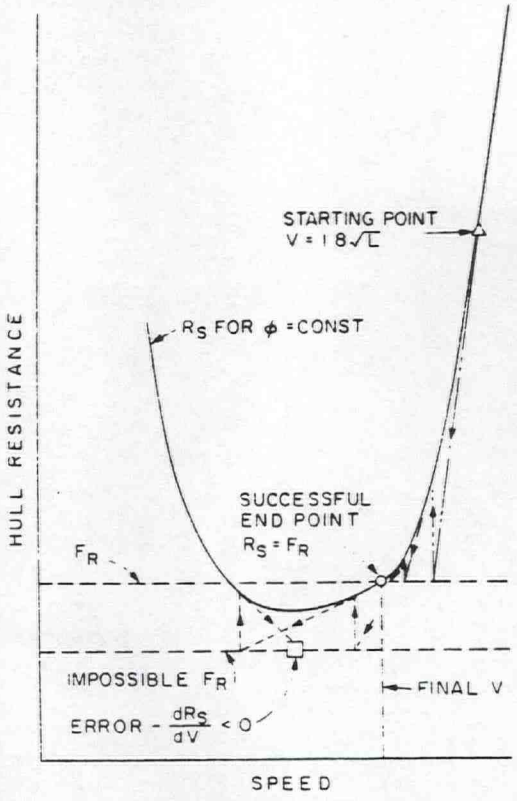

Figure 5. Schematic of iterative solution for boad speed.

note that in general there are two solutions, one corresponding to an efficient sailing condition and one characterized by a low speed accompanied by excessive induced drag. Both are physically valid solutions, and even a good helmsman might find himself temporarily in the low speed condition. The remedy, of course, is first to bear off, ease sheets and get moving, and then to "converge" to the high speed solution. The computer program must have the same characteristics, and this requires a built-in method of avoiding the wrong solution.

Since the hull drag function is approximated in each speed interval by a function which can be readily differentiated, the very efficient Newton-Raphson iterative method is employed:

$$V_{i+1} = V_i + \frac{F_R - R_{Si}}{\left(\frac{dR_S}{dV}\right)_i} \qquad (23)$$

where $F_R - R_{S_i}$ is the difference between the known sail driving force, F_R, and the computed hull resistance corresponding to the i-th trial value of boat speed, V_i. The derivative in (22) is the sum of the slope of the upright resistance curve

$$\frac{dR_T}{dV_i} = 3a_j(V_i - V_j)^2 + 2b_j(V_i - V_j) + c_j \qquad (24)$$

and the slopes of the heeled and induced resistance components

$$\frac{dR_H}{dV_i} + \frac{dR_I}{dV_i} = \frac{2(R_H - R_I)}{V_i} \qquad (25)$$

We begin the hull resistance iteration, not at the current boat speed, but at an artificially high speed/length ratio of 1.8. In this way we are sure to be on the right side of the resistance curve. We then obtain the first correction to speed from (23). Repeated application of (23) will generally lead to rapid convergence to the specified tolerance of 0.001 knots. If, for some reason, the iteration has not converged in 25 tries, an error flag is generated and the computation proceeds as though it had converged.

It is possible that the available driving force may be less than the minimum drag for the heel angle specified, as illustrated in Fig. (5). In this case, the iteration will move rapidly toward zero velocity, and would continue to negative velocities, if unconstrained.[2] A test is therefore made which completes the iteration if either a negative velocity or a negative value of dR_S/dV is encountered. No additional message is printed since it will be obvious from the printout that the imposed conditions are unrealistic. This condition is generally encountered only for relative wind angles substantially less than the optimum value for speed made good to windward.

Once the speed has converged for the prescribed driving force, we must repeat the entire process with a corrected initial assumed value of boat speed. If the apparent wind is forward of abeam, it has been found that the iteration converges rapidly if the assumed speed in the next trial is the speed which resulted from the driving force iteration. On the other hand, if the apparent wind is aft of abeam, this procedure diverges. The reason for this is that boat speed is more critical, of course, when running in light air. This convergence problem is solved by adding some damping to the iteration. If $\beta_{aw} > 90°$, the next assumed speed is the average of the input and output speeds of the preceding iteration. If $\beta_{aw} < 90°$, damping would unnecessarily slow down the convergence, and is therefore omitted. In either case, the complete iteration is terminated when the input and output speeds differ by less than 0.001 knots.

This iteration is also limited to 25 trials to prevent a costly computer run in the event of a diverging condition. Again, an error flag is generated and the computation continues.

If the heel angle obtained at this stage is less than the specified reefing angle, the computation of this sailing condition is now complete. However, if the converse is true, the entire computation is repeated with the reefing angle increased in one-degree increments until either

a) the reefing ratio becomes unity

b) the boat speed begins to decrease.

In the latter case, the optimum reefing angle is obtained from a parabolic fit to the three preceding computations

$$(\phi_R)_{opt} = (\phi_R)_{j-1} + \frac{1}{2}\,\frac{V_{j-2} - V_j}{V_{j-2} - 2V_{j-1} + V_j} \qquad (26)$$

when V_{j-2}, V_{j-1} and V_j are the equilibrium speeds obtained in the last three computations with one-degree increments in reefing angle. One final computation is then made with this value of the reefing angle. It should be noted that for apparent wind angles $\leq$ 48 degrees, the speed used in the optimization in (26) is the speed made good to windward. The actual boat speed is optimized for all apparent wind angles greater than 48 degrees.

This process is repeated for 16 values of true wind angle, ending with 34 degrees. The 17th computation is for the value of β_{tw} yielding the optimum speed made good to windward. This angle is also obtained by a parabolic fit to the three apparent wind angles bracketing the optimum, with an equation very similar to (26).

It is fortunate that this iterative process takes far longer to describe than to compute. The average computing time to obtain the converged solution with optimum reefing for a given true wind velocity and angle is approximately seven-thousandths of a second on the IBM 370/168 at M.I.T.

---

[2] The real world counterpart is "getting in irons."

This computing time would easily be increased by a factor of a hundred without the time-saving algorithms contained in the VPP.

RATING DIFFERENCES

In the evaluation of handicapping systems, it is frequently helpful to convert speed differences to rating differences. For example, it is a simple matter to obtain from the VPP the difference in speed resulting from a small change in stability. However, this speed difference cannot be compared directly with the corresponding rating difference which a given rule would assign to this change in stability.

We can define a "performance rating difference" as the rating difference relative to a selected scratch boat which results in equal corrected time according to a specified time allowance system. This performance rating difference will, in general, depend on wind velocity and direction, as well as on the time allowance system and the choice of the base rating.

For the NAYRU time-on-distance formula, used almost exclusively for ocean race handicapping in the United States, the corrected time, C, is obtained from the elapsed time, E, and the race distance, D, from the equation [10]

$$C = E + 0.6\ (R_{SC}^{-1/2} - R^{-1/2})d \qquad (27)$$

where R_{SC} is the scratch boat rating and R is the rating of the boat in question. If we set the corrected time equal to that of the scratch boat, and replace elapsed time by D/V we obtain the result

$$R-R_{SC} = \left[\frac{0.6}{V^{-1}-V_{SC}^{-1} + 0.6\ R_{SC}^{-1/2}}\right]^2 - R_{SC} \qquad (28)$$

If a time-on-time system is used, the result will be different. For example, the NAYRU time-on-time formula used in England for the 1975 Admiral's Cup [10] yields the result

$$R-R_{SC} = \left[\frac{1.0}{V^{-1} - V_{SC}^{-1} + R_{SC}^{-1/2}}\right]^2 - R_{SC} \qquad (29)$$

Both (28) and (29) have been incorporated in the VPP. The first boat computed in any run is, by definition, the scratch boat whose rating R_S must be specified. The velocities for all points of sailing for this boat are saved and are subsequently entered as V_{SC} when (28) and (29) are evaluated for all later boats. As in the determination of optimum reefing, speeds are interpreted as speeds made good to windward for $\beta_{tw} \leq 48$ degrees, and actual speeds for $\beta_{cw} > 48$. This causes a noticeable discontinuity in rating difference at 48 degrees, which is intentional. This does point out, however, the need to be careful in distinguishing between a dead beat and a close-hauled course for handicapping purposes.

ILLUSTRATIVE EXAMPLES

Calculations are given for several hypothetical yachts derived from the original lines 49-foot length overall sloop BAYBEA. The hull data are based on tank tests of a 4.7-foot model run at M.I.T. in 1967. Rig and inclining experiment data have been extracted from subsequent IOR certificates. The principal characteristics are given in Table 1.

Table 1. Principal Characteristics of Sample Yacht Based on BAYBEA

Length overall	49.09	ft
Test waterline length, L	35.92	
Wetted surface, S	427.6	ft
Test displacement, Δ	31.381	lbs
IOR Righting Moment	2129.5	ft-lbs/degree
Fore triangle height, I	61.42	ft
Fore triangle base, J	20.50	ft
Main triangle base, P	55.04	ft
Main triangle base, E	14.50	ft
Assumed center of effort	42% of mast height	

The resistance function as represented by equations (9) (10) and (12) is plotted in Fig. 6 for the BAYBEA hull scaled down, for convenience, to an even 35-foot waterline length. The simplified form of (13) using the IOR inclining result is used for stability since test data were not available to compute d_2 and d_3. The position of the center of effort of the side force, d_4L, was taken to be 35% of the draft below the waterline in accordance with results obtained experimentally for other hulls [8], [11]. This plot shows the resistance as a function of speed for one-degree increments of heel angle corresponding to values of stability and sail area scaled geometrically from the data of Table 1.

The same hull is shown in Fig. 7 with the stability reduced to 60% of the base value. While the upright resistance is obviously unchanged, the heeled resistance is much less, and takes on a completely different character. In particular, the minimum drag speed at each heel angle is considerably lower. One would expect, therefore, that the helmsman of the less stable boat would be not as likely to be trapped on the wrong side of the resistance curve. Conversely, an increase of

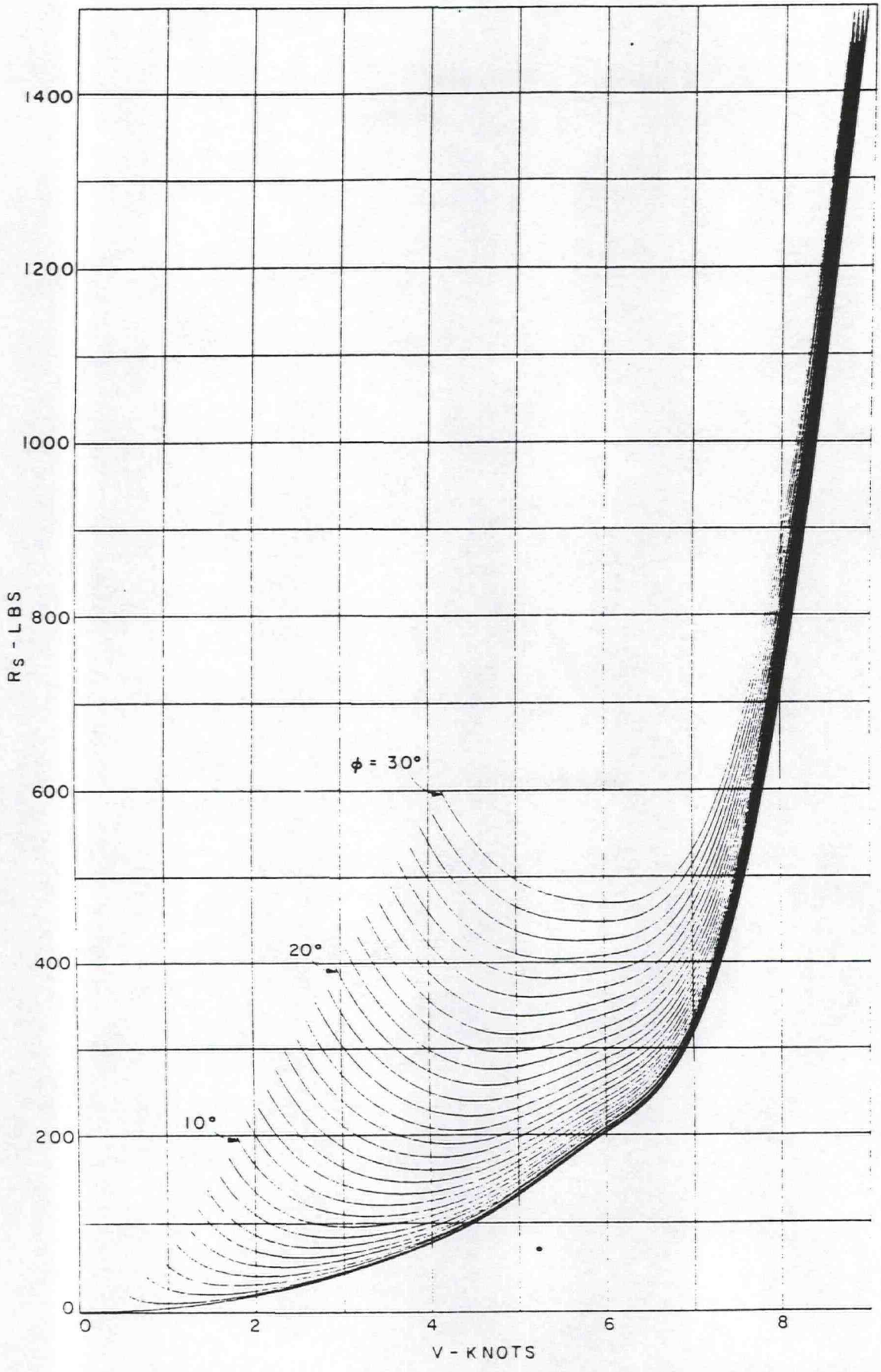

Figure 6. Resistance function for 35 ft. yacht with base stability.

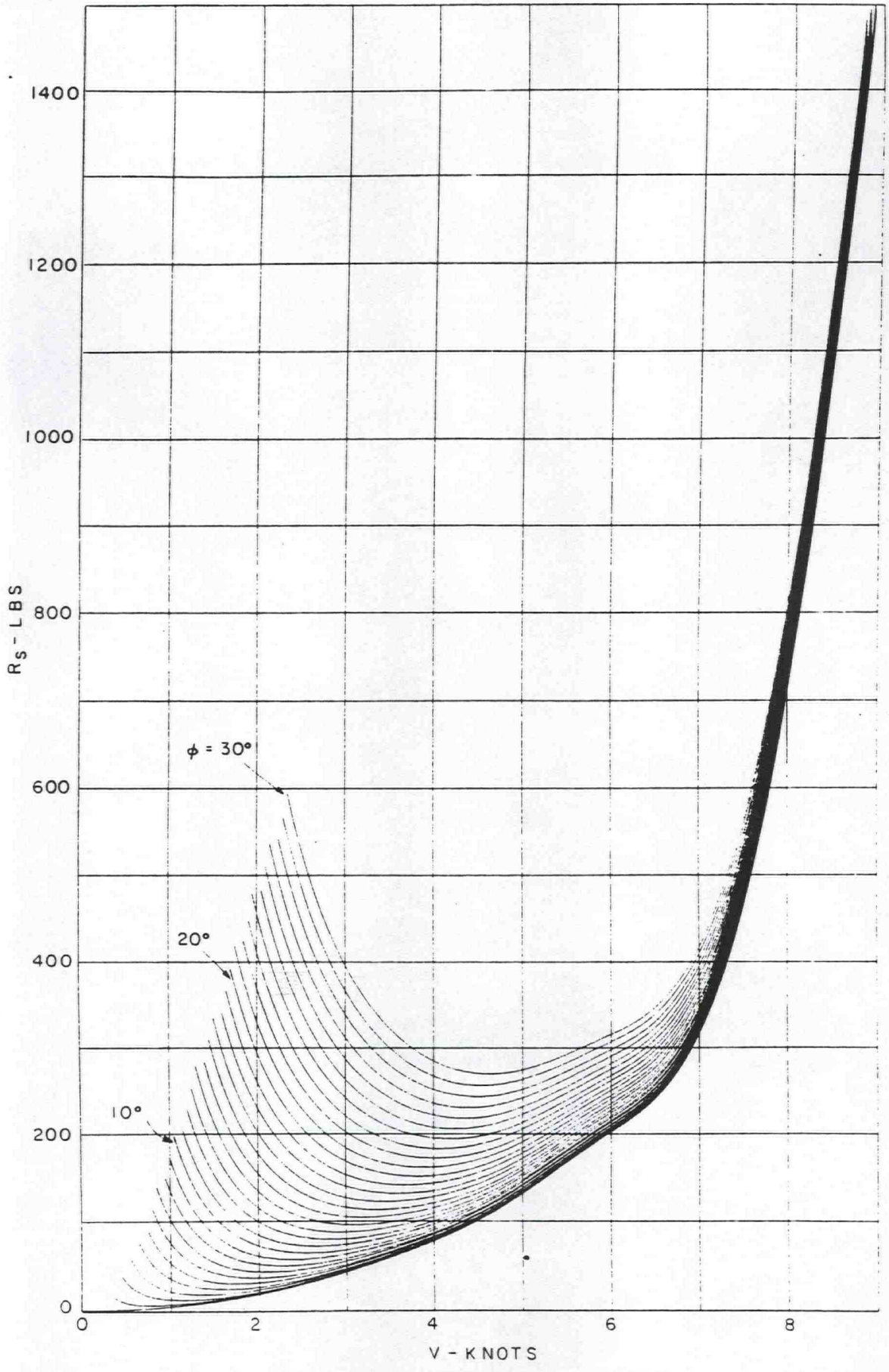

Figure 7. Resistance function for 35 ft. yacht with 60% of base stability.

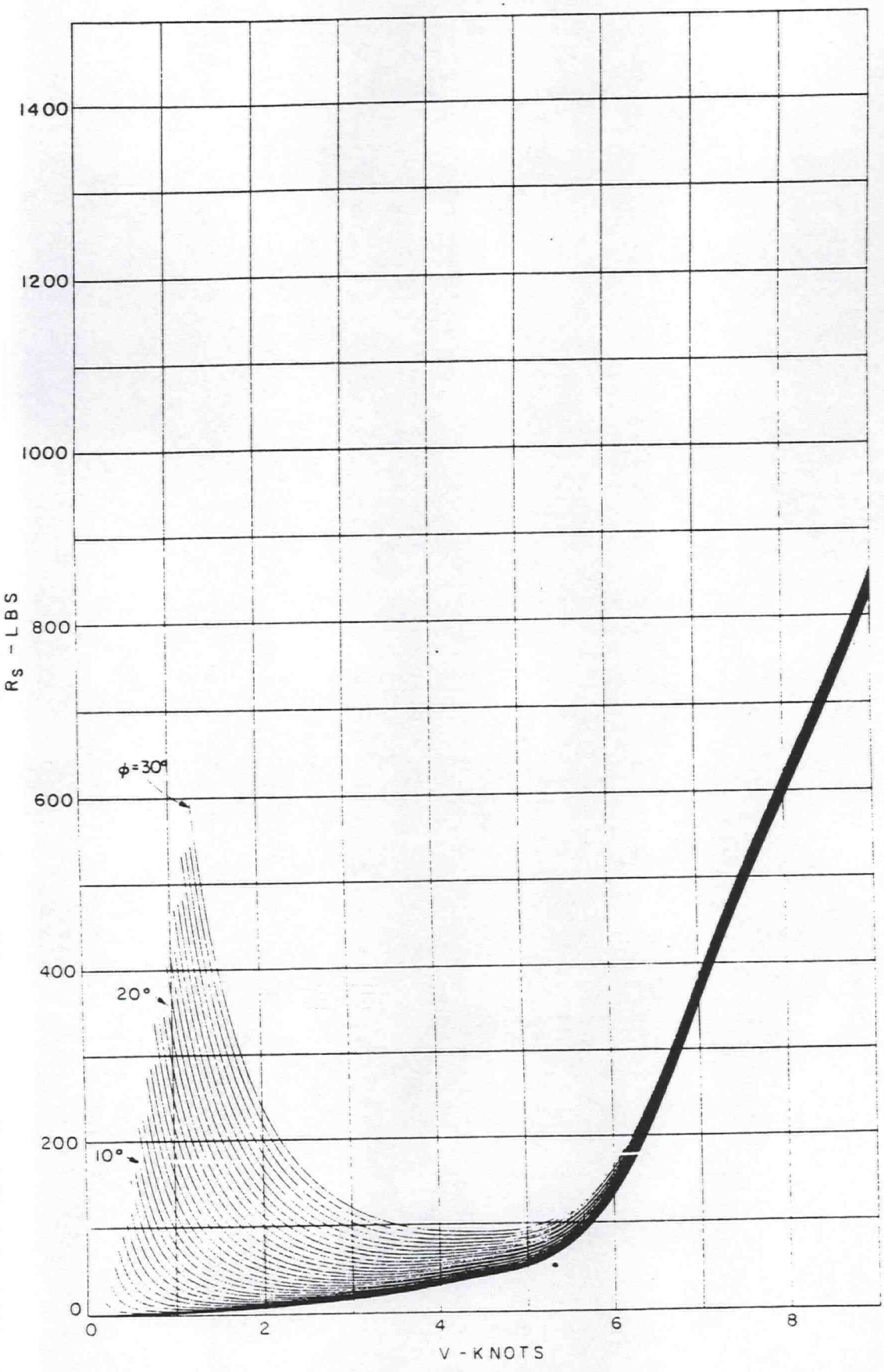

Figure 8. Resistance function for geometrically similar 20 ft. yacht with base stability.

stability increases the minimum drag speed, and tends to narrow the speed difference between the two solutions for constant resistance. Hence, a "lead mine" is much more demanding on the helmsman than the less stable boat in this particular respect.

Figure 8 shows the same hull again, but scaled down to a waterline length of 20 feet. The plot is made to the same scale in order to illustrate the effect of size on resistance at equal speeds.

Sample output from the VPP is shown in Table 2 for the 35-foot yacht with base stability for true wind velocities of 5, 10 and 20 knots. This output gives in great detail the final equilibrium values for each combination of wind speed and angle. The printed values of hull resistance can be compared with the data plotted in Fig. 6 for all sailing conditions where no reeding is present. If the reefing ratio, r, is less than one, the height of the center of effort of the rig is reduced so that Fig. 6 is no longer applicable.

Figs. 9 and 10 are examples of the type of analysis which can be performed with the VPP, using the rating difference output. In Fig. 9, we have plotted the performance rating difference of the 35-foot yacht resulting from a 20% change in sail area as a function of wind speed. The three solid curves represent the results for a boat, for a 100° true wind angle reach, and for a 170° true wind angle run. The horizontal dashed line represents the 2.7-foot rating increase in IOR rating which would result from this change in sail area. One can see from Fig. 9, for example, that in a 15-knot wind the yacht with more sail area can

TABLE 2

Sample VPP output for 35 ft. base yacht based on BAYBEA.

VT	B-TW	VA	B-AW	VB	VMG	PHI	REEF	FR	RI*RH	FR*COS(B)	CB/CV	TOD RTG DIFF	TOT RTG DIFF
5.0	180.0	2.67	180.00	2.327	-2.327	0.0	1.000	25.8	0.0	0.0	23.0	5.4	3.0
5.0	160.0	2.36	133.56	3.077	-2.888	7.4	1.000	46.0	0.1	25.6	30.5	3.6	2.1
5.0	140.0	3.23	88.87	4.119	-3.155	1.8	1.000	88.5	1.2	119.7	42.6	7.8	4.2
5.0	120.0	5.16	57.08	5.303	-2.652	5.2	1.000	160.5	7.1	352.2	70.3	6.9	3.3
5.0	100.0	7.18	43.29	6.095	-1.058	9.1	1.000	223.5	14.3	540.9	64.5	11.2	5.9
5.0	80.0	8.62	34.83	6.209	1.078	9.3	1.000	236.2	19.0	623.9	68.5	12.0	6.2
5.0	60.0	9.12	28.34	5.530	2.765	1.0	1.000	191.1	21.3	607.2	66.6	7.7	4.1
5.0	50.0	9.02	25.14	4.946	3.180	8.5	1.000	150.5	22.2	567.9	59.1	9.6	5.1
5.0	48.0	8.96	24.50	4.808	3.217	8.2	1.000	141.8	22.5	559.8	54.7	19.4	9.2
5.0	46.0	8.88	23.89	4.648	3.228	8.2	1.000	132.5	22.9	547.2	48.8	19.4	9.2
5.0	44.0	8.78	23.29	4.471	3.216	8.0	1.000	123.2	23.3	534.3	42.6	18.9	9.0
5.0	42.0	8.66	22.72	4.274	3.176	7.7	1.000	114.1	23.8	520.7	36.4	17.9	8.6
5.0	40.0	8.51	22.19	4.048	3.101	7.5	1.000	104.8	24.5	502.7	30.4	16.0	7.9
5.0	38.0	8.32	21.70	3.795	2.990	7.2	1.000	95.7	25.4	483.0	24.7	14.4	7.2
5.0	36.0	8.11	21.25	3.517	2.846	6.8	1.000	86.9	26.6	461.9	19.9	*****	*****
5.0	34.0	8.03	20.19	2.712	2.249	6.7	1.000	77.0	42.6	458.5	-4.0	*****	*****
5.0	46.0	8.88	23.90	4.650	3.228	8.2	1.000	132.6	22.8	547.2	48.9	19.3	9.3
10.0	180.0	5.41	180.00	4.585	-4.585	0.0	1.000	106.1	0.0	0.0	55.5	4.0	2.3
10.0	160.0	4.32	135.94	5.863	-5.510	1.5	1.000	194.1	0.5	102.9	68.5	5.2	2.9
10.0	140.0	6.46	95.33	7.061	-5.409	5.4	1.000	335.6	5.3	369.7	226.4	12.4	6.3
10.0	120.0	9.04	73.32	7.595	-3.798	13.2	1.000	533.8	32.3	874.9	421.9	14.2	7.1
10.0	100.0	11.55	58.48	7.777	-1.350	20.2	1.000	670.2	83.8	1281.2	498.9	15.5	7.6
10.0	80.0	13.69	46.01	7.771	1.349	23.3	1.000	702.6	119.6	1451.3	489.8	16.9	8.2
10.0	60.0	15.26	34.58	7.565	3.783	22.7	1.000	604.3	115.4	1418.7	395.0	17.2	8.4
10.0	50.0	15.71	29.18	7.287	4.644	21.7	1.000	497.7	107.8	1365.7	294.3	17.2	8.4
10.0	48.0	15.76	28.14	7.202	4.819	21.5	1.000	472.1	106.6	1353.6	251.8	15.4	14.9
10.0	46.0	15.78	27.12	7.101	4.933	21.1	1.000	445.3	105.7	1344.1	220.2	12.8	13.8
10.0	44.0	15.78	26.12	6.972	5.015	21.0	1.000	416.5	105.2	1328.3	191.5	10.2	13.0
10.0	42.0	15.74	25.17	6.811	5.062	20.7	1.000	387.4	105.0	1313.5	139.6	27.8	12.2
10.0	40.0	15.63	24.28	6.591	5.049	20.4	1.000	357.6	105.6	1292.8	93.6	24.9	11.2
10.0	38.0	15.43	23.52	6.268	4.939	19.9	1.000	328.8	107.2	1266.1	50.9	21.0	9.8
10.0	36.0	15.14	22.84	5.775	4.672	19.3	1.000	300.4	113.0	1232.2	38.3	*****	*****
10.0	34.0	15.97	20.50	-0.048	-0.040	20.7	1.000	254.5	169.2	1315.7	10.1	-20.0	-20.0
10.0	41.4	15.72	24.90	6.757	5.066	20.6	1.000	379.1	105.1	1309.0	126.9	25.4	11.4
20.0	180.0	12.30	180.00	7.698	-7.698	0.0	1.000	547.3	0.0	0.0	471.9	10.2	5.4
20.0	160.0	12.40	146.52	8.453	-7.943	6.5	1.000	1059.9	6.4	432.3	881.1	9.2	4.9
20.0	140.0	14.38	116.65	8.869	-6.794	15.1	1.000	1493.3	39.3	996.6	1023.3	8.8	4.7
20.0	120.0	17.35	93.27	9.011	-4.506	27.3	1.000	1756.0	153.8	1643.7	1034.7	11.1	5.8
20.0	100.0	20.39	75.04	8.736	-1.517	30.0	0.861	1568.2	247.4	2050.4	962.4	13.3	7.0
20.0	80.0	23.03	58.79	8.460	1.469	30.0	0.774	1364.1	304.5	2240.0	838.1	15.9	7.8
20.0	60.0	25.15	43.52	8.237	4.118	30.0	0.775	1190.8	314.9	2277.6	707.6	17.5	8.5
20.0	50.0	25.94	36.20	8.075	5.191	30.0	0.803	1065.5	304.7	2197.9	614.1	17.9	8.6
20.0	48.0	26.06	34.77	8.026	5.371	30.0	0.810	1031.3	302.9	2179.2	586.9	17.4	15.2
20.0	46.0	26.17	33.35	7.969	5.536	30.0	0.817	994.8	301.4	2160.2	555.7	14.9	14.4
20.0	44.0	26.26	31.94	7.900	5.683	30.0	0.824	953.3	300.5	2141.1	518.4	12.7	13.3
20.0	42.0	26.34	30.54	7.819	5.811	30.0	0.832	908.4	300.3	2122.5	476.7	11.0	13.2
20.0	40.0	26.38	29.16	7.719	5.913	30.0	0.839	858.9	301.3	2104.2	427.2	29.5	12.8
20.0	38.0	26.40	27.80	7.595	5.985	30.0	0.846	805.3	303.9	2086.6	368.2	28.3	12.4
20.0	36.0	26.38	26.47	7.433	6.013	30.0	0.853	747.2	309.1	2069.5	296.8	27.3	12.0
20.0	34.0	26.31	25.15	7.235	5.999	29.2	0.765	600.3	225.2	1955.9	236.0	26.5	11.8
20.0	35.7	26.37	26.25	7.403	6.014	27.6	0.816	731.1	273.5	2039.2	291.0	26.9	11.9

NOTE: If solution has not converged, the symbol ***** is printed in place of rating differences. Note that these only occur for wind angles less than the optimum.

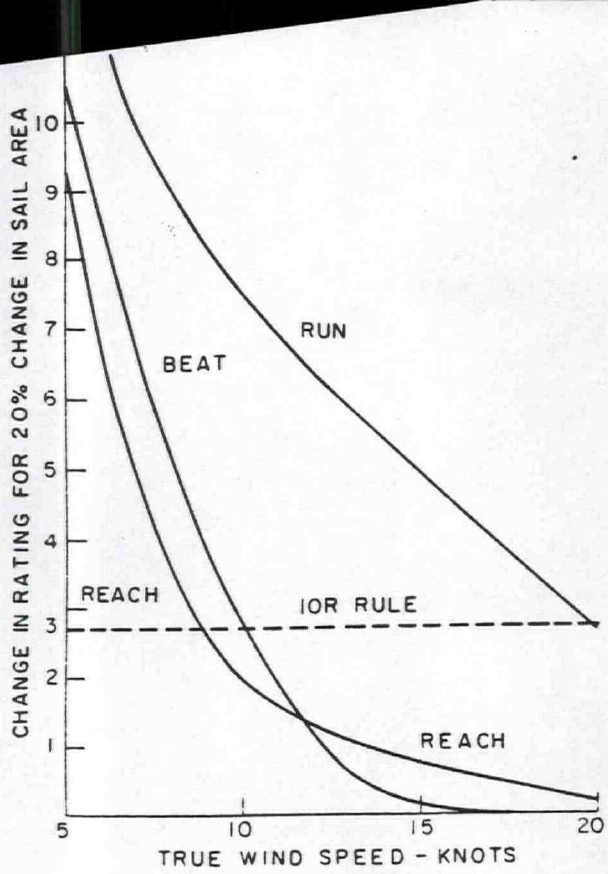

Figure 9. Influence of sail area on performance rating using NAYRU time-on distance time allowance formula

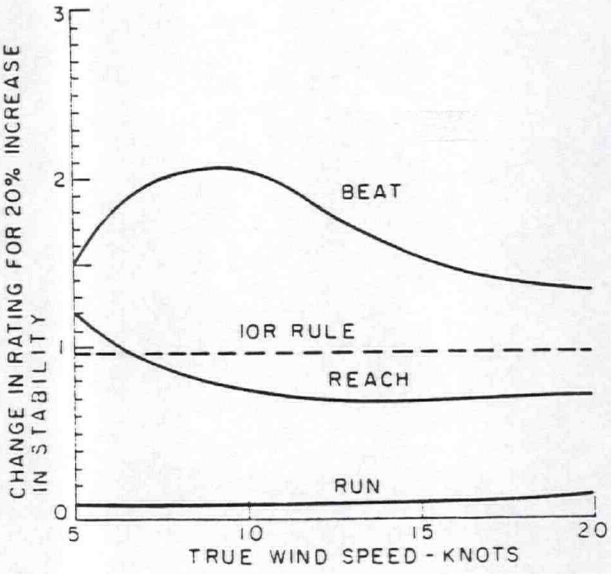

Figure 10. Influence of stability on performance rating using NAYRU time-on distance time allowance formula.

afford to rate 4.8 feet higher on a run, but only 0.1 feet higher on a boat. Hence, the IOR rule increase of 2.7 feet would be too little to account for the increased running speed, too much to account for the increased windward performance, and just about right on the average for a windward-leeward race. On the other hand, in a light 5-knot breeze the performance rating increase far exceeds the rule increase on all points of sailing, and the converse is true in winds of 20 knots or higher. This illustrates the impossibility of characterizing the speed of a yacht under varying wind speeds and points of sailing by a single rating and time allowance system. Rating inequities for a particular point of sail far exceed the differences between existing or proposed rating rule formulation.

Another example of performance rating differences is given in Fig. 10. In this case, the sail area has been kept constant and the stability has been increased by 20%. As would be expected, the performance on a boat exceeds the IOR expectation, while on a run it is essentially unchanged. What is surprising is that the windward performance rating increase is greater in a 10-knot than in a 20-knot wind. The explanation can be found, in part, from a comparison of Figs. 9 and 10. In very light air, small speed differences generate late time differences due to the fact that speeds are low and elapsed times are large. In that case, anything that increases speed will exceed the expectation of the rating rule. On the other hand, in heavy air speed increases are harder to develop owing to the steep rise in the hull resistance curve at high speeds. Consequently, performance ratings, both due to sail area and stability, tend to become less at higher speeds. As we approach low wind velocities, both performance ratings increase. However, when heel angles become sufficiently small, the influence of speed on stability disappears so that the performance rating due to stability starts to go back down again. This is, of course, not true with the sail area so that the curves in Fig. 9 rise continually with decreasing wind velocity.

Figures 11-13 show the results of the calculation of a geometrically similar fleet of yachts derived from BAYBEA, with waterline lengths varying from 20 to 70 feet. The plots show the performance rating difference relative to the 20-foot "scratch" boat for three different points of sailing. Separate plots are made for three different wind velocities.

These graphs show the extent to which the effect os size is dependent on

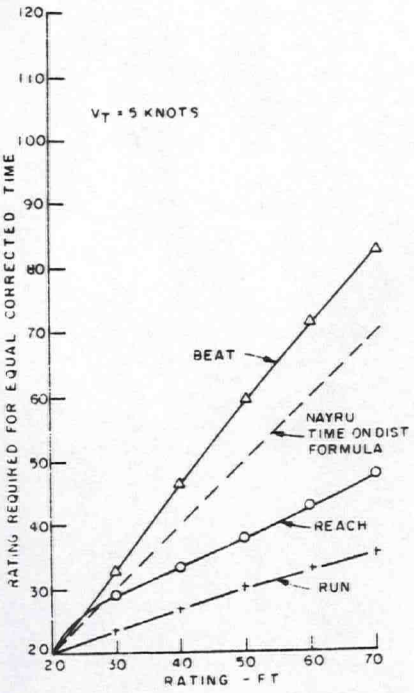

Figure 11. Effect of size on performance rating in 5 knot wind.

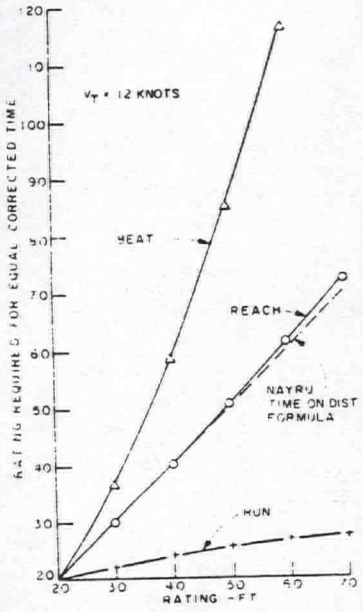

Figure 12. Effect of size on performance rating in 12 knot wind.

the particular sailing conditions encountered in a race. In these graphs the run is a dead run chosen to emphasize the plight of the large yacht running out of apparent wind. If we had plotted instead the performance rating corresponding to maximum speed made good to leeward achieved by tacking downwind, the large yacht would not look quite as bad. The situation is reversed going to windward where the large yacht is at a gread disadvantage.

In studying these results, it is

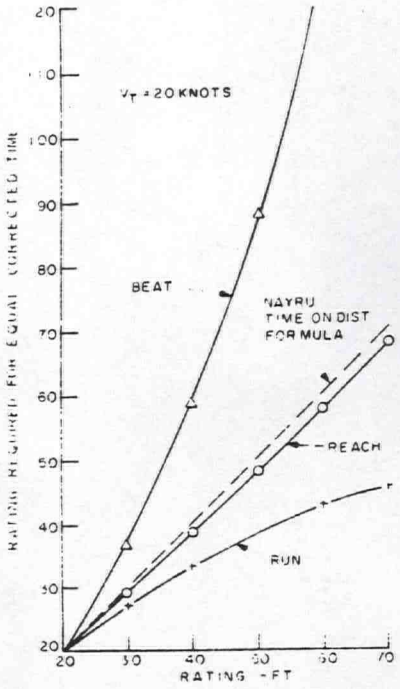

Figure 13. Effect of size on performance rating in 20 knot wind.

important to keep in mind that performance rating differences are not absolute, but depend on the scratch rating, as is evident from (28). The trends, however, are the same regardless of the choice of scratch rating.

These results are provided strictly as examples of the kind of information which can be provided by the VPP. More extensive plots of VPP speed prediction for yachts of varying size and sail area may be found in [12], and a comprehensive study of the influence of the major speed-producing characteristics of a yacht is now underway.

ACKNOWLEDGEMENTS

This research was carried out under the North American Yacht Racing Union Ocean Race Handicapping Project, M.I.T. OSP Project No. 81535. The generous support of the individual donors to this program is gratefully acknowledged.

REFERENCES

[1] Hazen, G., "Analysis of the 1975 New York Yacht Club Cruise Data with Conventional and Variable Rating Time Allowance Systems", *New England Sailing Yacht Symposium*, New London, Conn., Jan., 1976.

[2] Davidson, K. S. M., "Some Experimental Studies on the Sailing Yacht", *Trans. Soc. of Nav. Archs. & Marine Engineers*, Vol. 44, 1936.

[3] Milgram, J., "The Analytical Design of Yacht Sails", *Trans. Soc. of Nav. Archs. & Marine Engineers*, Vol. 76, 1968.

[4] Milgram, J., "Sail Force Coefficients for Systematic Rig Variations", *Soc. of Nav. Archs. & Marine Engineers*, T & R Report R-10, 1971.

[5] Marchaj, C., "Wind Tunnel Tests of a 1/4-Scale Dragon Rig", Univ. of Southamption, Dept. of Aeronautics, SUYR Paper No. 14, 1964.

[6] Spens, P. G., DeSaix, Pierre, and Brown, P. W., "Some Further Experimental Studies of the Sailing Yacht", *Trans. Soc. of Nav. Archs. & Marine Engineers*, Vol. 75, 1967.

[7] Kerwin, J. E., Oppenheim, B. W., and Mays, J. H., "A Procedure for Sailing Performance Analysis Based on Full Scale Log Entries and Towing Tank Data", MIT, Dept. of Ocean Engineering, Report No. 74-17, July, 1974.

[8] Gerritsma, J., Kerwin, J. E., and Moeyes, G., "Determination of Sail Forces Based on Full Scale Measurements and Model Tests", *4th HISWA Symposium*, Amsterdam, Nov., 1975.

[9] Herreshoff, H. C., "Hydrodynamics and Aerodynamics of the Sailing Yacht", *Trans. Soc. of Nav. Archs. & Marine Engineers*, Vol. 2, 1964.

[10] Newman, J. N. and Hazen, G. S., "Race Statistics and Time Allowance Comparisons", MIT, Dept. of Ocean Engineering, Report 75-2, Feb., 1975.

[11] Beukelman, W. and Keuning, J. A., "The Influence of Fin Keel Sweep-Back on the Performance of Sailing Yachts", *4th HISWA Symposium*, Amsterdam, Nov., 1975.

[12] Newman, J. N., "Handicapping Systems for Ocean Racing Yachts", *The Naval Architect*, July, 1975.